Cycling performance of lithium-ion polymer batteries assembled using in-situ chemical cross-linking without a free radical initiator

CrossMark

Young-Woo Lee [a,b], Won-Kyung Shin [a], Dong-Won Kim [a,*]

[a] Department of Chemical Engineering, Hanyang University, Seoul 133-791, Republic of Korea
[b] Cell Development Group, Samsung SDI, Chungcheongnam-do 331-710, Republic of Korea

ARTICLE INFO

ABSTRACT

We present a cross-linked gel polymer electrolyte for lithium-ion polymer batteries that can be easily synthesised without any initiators. The gel polymer electrolyte has a high ionic conductivity comparable to a liquid electrolyte, as well as favourable interfacial characteristics between the electrodes and the electrolyte during cycling. The lithium-ion polymer batteries assembled with cross-linked gel polymer electrolyte exhibit improved capacity retention and good rate capability.

© 2013 Elsevier B.V. All rights reserved.

1. Introduction

Due to their high energy density and long cycle life, lithium-ion batteries have become the dominant power sources for portable electronic devices and electric vehicles [1,2]. However, safety issues still prevent full utilisation of these batteries. The high flammability of the organic solvents used in liquid electrolytes can lead to fires and explosions when short circuits or local overheating accidentally occurs. Therefore, there is a pressing need for safer, more reliable electrolyte systems, and polymer electrolytes are promising candidates in this regard [3–10]. Solid polymer electrolytes based on poly(ethylene oxide) are the most common examples. However, their low ionic conductivities, ranging from 10^{-8} to 10^{-5} S cm^{-1}, preclude their practical application for use in rechargeable lithium batteries at ambient temperatures. Accordingly, the most relevant research has focused on gel polymer electrolytes that exhibit higher ionic conductivities at room temperature. Such gel polymer electrolytes encapsulate a large number of liquid electrolytes in host polymers, such as polyacrylonitrile, poly(vinylidene fluoride-co-hexafluoropropylene) and poly(methyl methacrylate), and their ionic conductivities usually exceed 10^{-3} S cm^{-1}, which is necessary for practical battery applications. Nevertheless, most efforts to increase the ionic conductivity by incorporating larger numbers of liquid electrolytes have been detrimental to their mechanical properties. An in-situ chemical cross-linking method with a multi-functional acrylate has been used to overcome this problem [11–16]; this technique has been applied to the manufacture of commercialized lithium-ion polymer batteries. In this process, an electrolyte solution containing cross-linking agents is injected into a lithium-ion cell, and gelation is carried out by heating the cell. However, this method has inherent disadvantages. The thermal curing procedure generally uses free radical initiators and must occur at an elevated temperature, which may induce thermal decomposition of the salt, formation of bubbles in the gel electrolyte due to gas evolution by thermal decomposition of initiator such as azobisisobutyronitrile (AIBN) and solvent evaporation. These factors can ultimately lead to degradation in battery performance [17,18]. Thus, there is great interest in an in-situ cross-linking approach that does not require the use of thermal initiators.

In this study, a cross-linked gel polymer electrolyte was synthesised without any initiators. As cross-linking agents, we used polyethyleneimine (PEI) with amine groups and poly(ethylene glycol) diglycidyl ether (PEGDE) with epoxy groups. Previously, our group has reported the cross-linking reaction of PEI with PEGDE for applications in dye-sensitised solar cells [19,20]. In this paper, the cycling performance of lithium-ion polymer batteries assembled by in-situ chemical cross-linking was investigated and compared with that of liquid electrolyte-based lithium-ion batteries. Our results confirmed the superior performance of the cross-linked gel polymer electrolyte compared with liquid electrolyte.

2. Experimental

2.1. Materials

PEI (branched, $M_n = 10,000$) and PEGDE ($M_n = 500$) (Aldrich Chemical Co.) underwent vacuum drying at 90 °C for 4 h and 50 °C for

4 h, respectively. A liquid electrolyte, which consisted of 1.3 M LiPF$_6$ in ethylene carbonate(EC)/propylene carbonate(PC)/ethyl propionate(EP) (3:1:6 by volume, battery grade) containing 3 wt.% fluoroethylene carbonate (FEC), was kindly supplied by Panax-Etec. Co., and was used without further treatment. The water content in the liquid electrolyte was determined to be less than 20 ppm by Karl Fisher titration.

2.2. Preparation of the gel polymer electrolytes and cell assembly

Fig. 1 illustrates the synthetic scheme of the cross-linked gel polymer electrolyte. The gel electrolyte precursor consisted of PEI, PEGDE and the liquid electrolyte. A mixture of PEI and PEGDE was added to the liquid electrolyte at a concentration of 1 wt.%, and the solution was stored at ambient temperature. The ratio of PEI to PEGDE was fixed to be 7:3 by weight. After 12 h, fluorinated carbamate was obtained through a reaction between PEI and FEC, as shown in Fig. 1(a). To induce the crosslinking reaction of fluorinated carbamate with reactive epoxy groups in PEGDE, the solution was heated to 65 °C and maintained at that temperature for 4 h. The cross-linked gel polymer electrolyte was then obtained by the ring-opening reaction of PEGDE with fluorinated carbamate (Fig. 1(b)). Note that no gas was evolved in the gel polymer electrolyte during the cross-linking reaction at 65 °C. The LiCoO$_2$ electrode was prepared by coating an n-methyl pyrrolidone (NMP)-based slurry containing LiCoO$_2$ (Japan Chemical), poly(vinylidene fluoride) (PVdF) and super-P carbon (MMM Co.) (85:7.5:7.5 by weight) onto
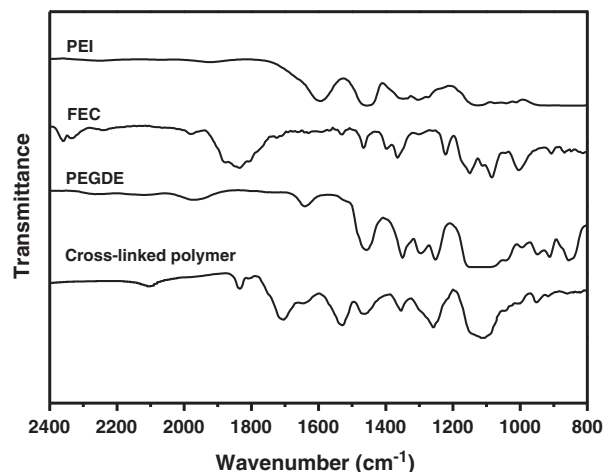

Fig. 2. FT-IR spectra of PEI, FEC, PEGDE and cross-linked polymers obtained from the thermal cross-linking reaction of the PEI, FEC and PEGDE mixture.

an aluminium foil. Its active mass loading corresponded to a capacity of about 2.6 mAh cm^{-2}. The carbon electrode was prepared in a similar manner by coating an NMP-based slurry of mesocarbon microbeads (MCMB, Osaka gas), PVdF and super-P carbon (88:8:4 by weight) onto
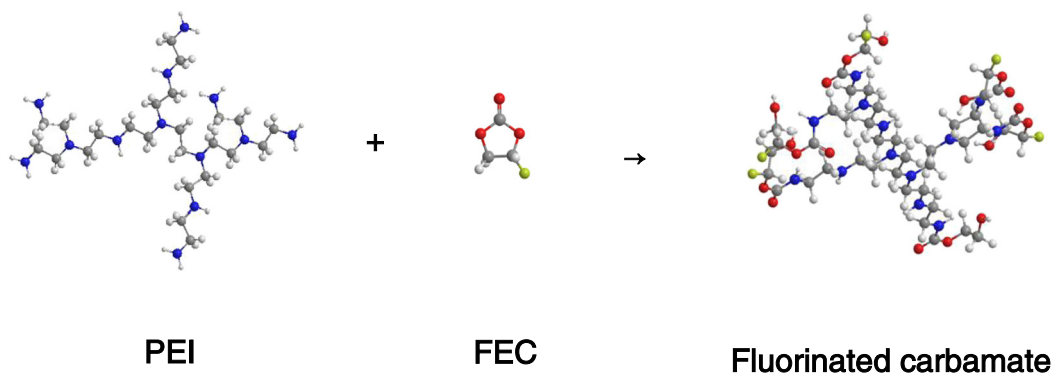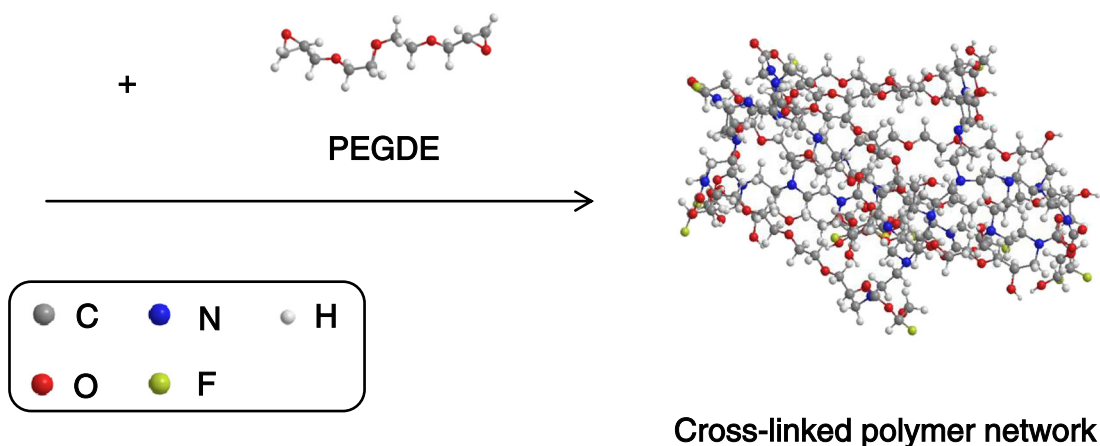

Fig. 1. Reaction scheme for synthesis of a cross-linked polymer network. (a) Fluorinated carbamate synthesised from the reaction between PEI and FEC, and (b) cross-linked polymer network obtained by ring-opening reaction between fluorinated carbamate and PEGDE.
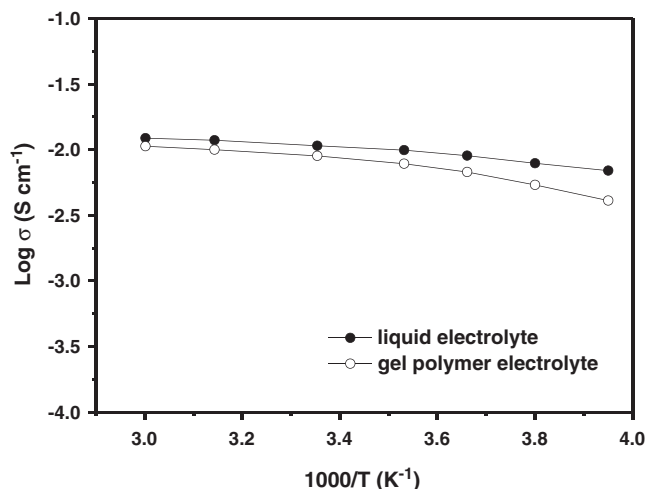
Fig. 3. Temperature dependence of ionic conductivity for liquid electrolyte and gel polymer electrolyte.

2.3. Measurements

Fourier-transform infrared (FT-IR) spectra were recorded on a Magna IR 760 spectrometer in the range of 400–4000 cm^{-1} with KBr powder-pressed pellets. The morphologies of the electrodes were examined using field-emission scanning electron microscopy (FE-SEM, JEOL JSM-6330F). The viscosities of the electrolyte systems were measured using a viscometer (Schott AVS 350). The ionic conductivity of the liquid electrolyte was measured by a Cond 3210 conductivity metre (WTW GmbH, Germany), and the ionic conductivity of the cross-linked gel polymer electrolyte after thermal curing was determined from AC impedance measurements. AC impedance measurements were performed using an impedance analyser over a frequency range of 1 mHz to 100 kHz with an amplitude of 10 mV. Charge and discharge cycling tests of the lithium-ion polymer batteries were conducted over a voltage range of 3.0–4.2 V with a battery cycler. Chracterization of the solid electrolyte interphase (SEI) formed on the carbon negative electrodes after charge–discharge cycling was performed by X-ray photoelectron spectroscopy (XPS) measurements (ESCA 2000, Thermo VG Scientific). To accomplish this measurement, the pouch cells were disassembled in the dry box, and small pieces of the electrodes were directly mounted onto the XPS sample holders. The samples were moved to the XPS analysis equipment while maintaining an Ar atmosphere. The samples encountered no atmospheric contamination during transportation to the XPS instrument and the XPS measurements.

a copper foil. The lithium-ion cell was assembled using a jelly roll, composed of a carbon negative electrode, a polyethylene separator (ND 420, Asahi) and a LiCoO$_2$ positive electrode. The jelly roll was enclosed in a pouch bag. It was injected along with the gel electrolyte precursor, and then vacuum-sealed. Cell assembly was carried out in a dry box filled with argon gas. To induce in-situ thermal curing of the gel electrolyte precursor, the cell was kept at 25 °C for 12 h, followed by additional ageing at 65 °C for 4 h. The nominal capacity of the cell was estimated to be about 600 mAh.

3. Results and discussion

FT-IR analysis was carried out to confirm the chemical cross-linking reaction among PEI, FEC and PEGDE, and the resulting FT-IR spectra are shown in Fig. 2. After thermal curing, the cross-linked polymer
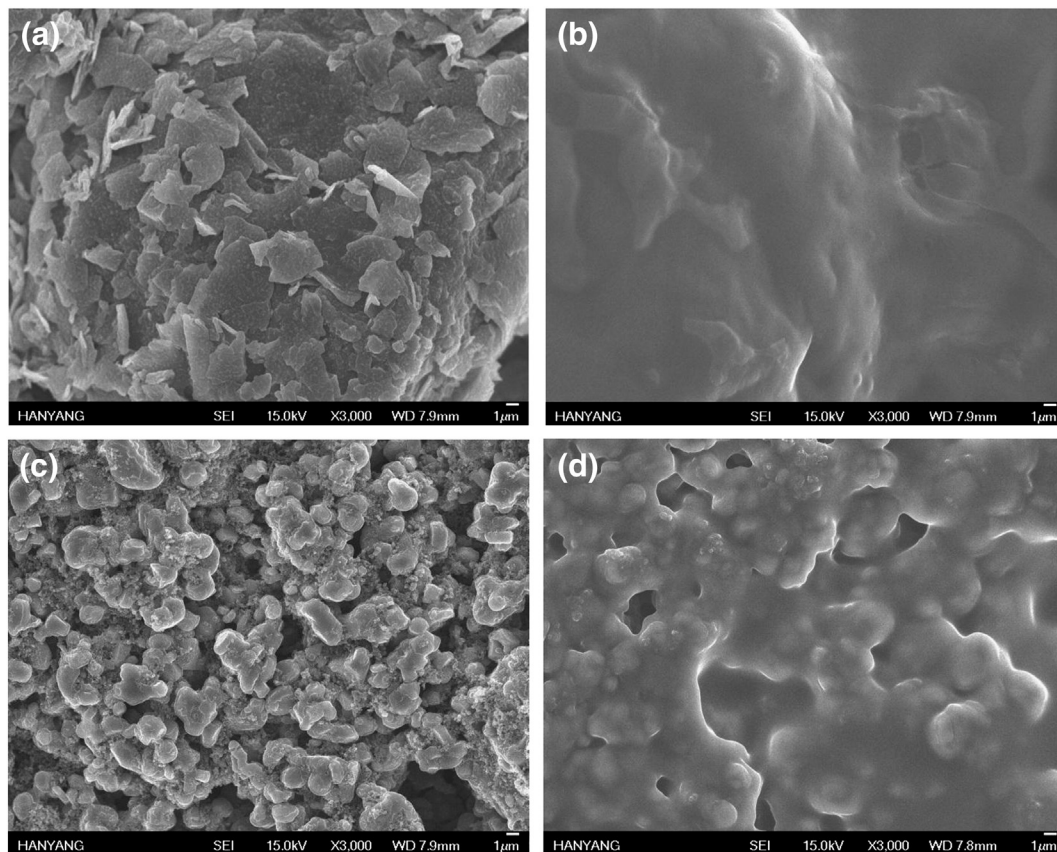

Fig. 4. FE-SEM images of the electrodes in cells assembled with the liquid electrolyte and the cross-linked gel polymer electrolyte: (a) negative electrode in the liquid electrolyte, (b) negative electrode in the gel polymer electrolyte, (c) positive electrode in the liquid electrolyte, and (d) positive electrode in the gel polymer electrolyte.

exhibited two additional peaks at 1705 and 1520 cm^{-1}, which are the characteristic peaks of the carbamate groups including the C–N–H bond [21–23]. This result suggests that the carbamate was formed by the reaction between amine group in PEI and carbonate in FEC. Synthesis of carbamate from amine and carbonate has been reported in greater detail in previous studies [24]. In the current study, we found that the characteristic peaks of the epoxy groups [25] in PEGDE at 911 and 844 cm^{-1} disappeared in the cross-linked polymer, indicating that the epoxy groups reacted with the amine groups to form a cross-linked polymer network [19,20,26]. Thus, the FT-IR results indicated that FEC reacted with PEI to form fluorinated carbamate, and that the carbamate participated in the ring-opening reaction of the epoxide in PEGDE by thermal treatment. As a result, a gel polymer electrolyte without flow was obtained after chemical cross-linking reaction.

Fig. 3 shows the temperature dependence of ionic conductivity for liquid electrolyte and gel polymer electrolyte, over the temperature range from −20 to 60 °C. The cross-linked gel polymer electrolyte exhibited a high ionic conductivity of 9.0×10^{-3} S cm^{-1} at 25 °C, which was much higher than those of other gel polymer electrolyte systems [5]. The ionic conductivity of the liquid electrolyte used in preparing gel polymer electrolyte was 1.1×10^{-2} S cm^{-1} at the same temperature. Difference in ionic conductivities between liquid electrolyte and gel polymer electrolyte slightly increased with decreasing

temperature, which can be ascribed to the reduction of ionic mobility due to the hindered segment motion of polymer chain at low temperature.

Gel formation was confirmed by observing the electrode surface after disassembling the cells. Fig. 4 shows FE-SEM images of the surface morphologies of electrodes in the cells assembled with the liquid electrolyte and the cross-linked gel polymer electrolyte, which were obtained before executing the cycling test of the batteries. Clearly, both the carbon negative electrode and the LiCoO$_2$ positive electrode in the cell assembled by in-situ chemical cross-linking were covered by the gel polymer electrolyte layer, indicating that the cross-linking reaction was carried out without any initiators in the cell.

The cycling performance of the lithium-ion polymer battery assembled with the cross-linked gel polymer electrolyte was evaluated. The assembled batteries were initially subjected to a preconditioning cycle over the voltage range of 3.0–4.2 V at a constant current of 60 mA (0.1C rate). After two cycles at the 0.1C rate, the batteries were charged at 300 mA (0.5C) up to a set voltage of 4.2 V, followed by a constant voltage charge until the final current reached 10% of the charging current. The batteries were then discharged down to a cut-off voltage of 3.0 V at the same current (300 mA, 0.5C). Fig. 4(a) shows a typical voltage profile of the 1st, 50th, 100th, 200th and 300th charge–discharge cycles of the lithium-ion polymer battery assembled with the cross-linked gel polymer electrolyte. The battery initially delivered a discharge
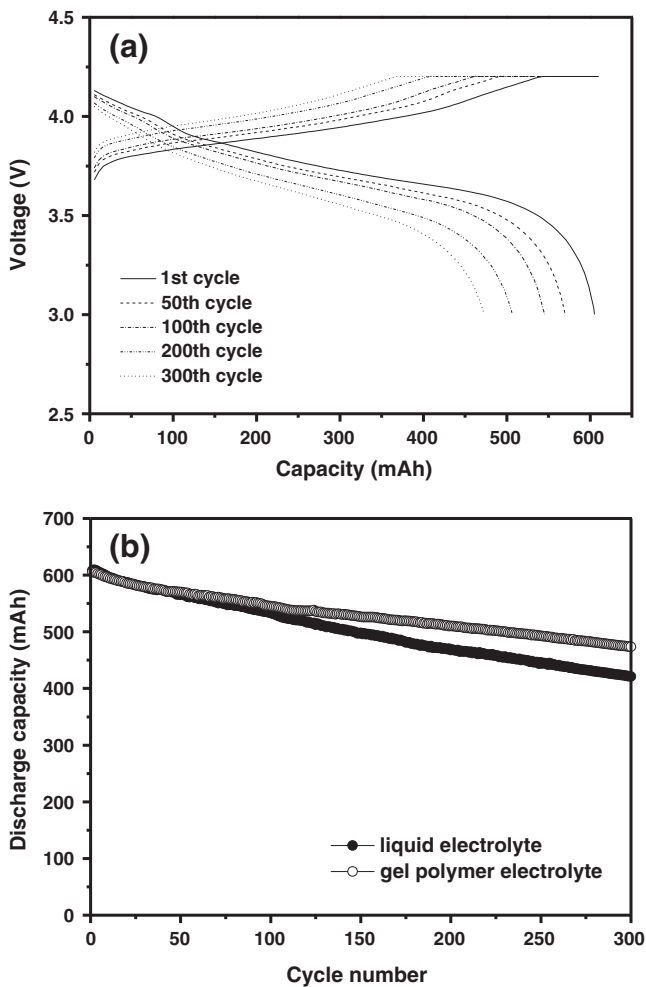

Fig. 5. (a) Voltage profile of the 1st, 50th, 100th, 200th and 300th charge–discharge cycles of the lithium-ion polymer battery assembled with the cross-linked gel polymer electrolyte, and (b) discharge capacity as a function of the cycle number in the batteries prepared with the liquid electrolyte and the cross-linked gel polymer electrolyte. Cycling was carried out between 3.0 and 4.2 V at 0.5C rate and 25 °C.
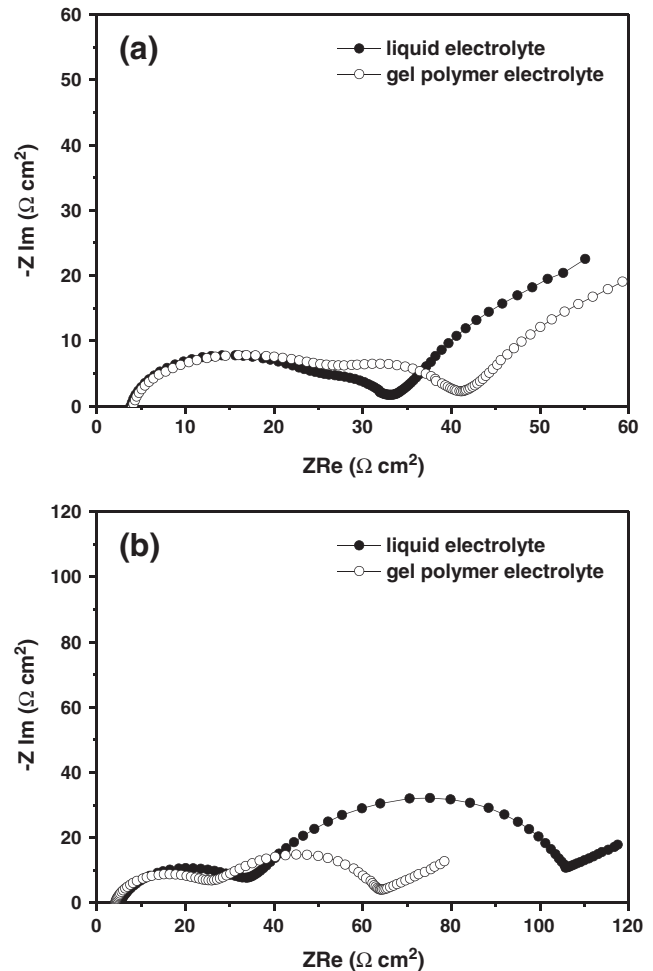

Fig. 6. AC impedance spectra of the batteries assembled with the liquid electrolyte and cross-linked gel polymer electrolyte (a) after the pre-conditioning cycles and (b) after 300 cycles.

capacity of 605.2 mAh. The discharge capacity decreased to 473.3 mAh at the 300th cycle, corresponding to 78.2% of the initial value. The coulombic efficiency steadily increased and stabilised with the cycle number, and was maintained at >99.5% throughout cycling after the first few initial cycles. Fig. 5(b) shows the discharge capacity as a function of the cycle number in the batteries prepared with the liquid electrolyte and the cross-linked gel polymer electrolyte. Obviously, the capacity retention improved in the battery with the cross-linked gel polymer electrolyte. Note that the compact interfacial contact between the polyethylene separator and the electrodes should be maintained during cycling for stable capacity retention. Upon gelation of the liquid electrolyte by thermal curing with the cross-linking agent, it became a gel polymer network and served as an adhesive, chemically bonding the separator and the electrodes, resulting in good capacity retention. The ability to retain the electrolyte solution in the cell was also favoured by the cross-linking of the liquid electrolyte, which helped to prevent exudation of the electrolyte solution during cycling.

Fig. 6 shows the AC impedance spectra of the batteries obtained at the charged state after the pre-conditioning cycle and at the charged state after 300 cycles. All of the spectra exhibited two overlapping semicircles, which were assigned to the resistance of Li^+ ions through the SEI film (R_f) at the electrode surface, and the charge transfer resistance at the electrode–electrolyte interface (R_{ct}) [27,28]. As shown in Fig. 5(a), the electrolyte resistances (R_e) estimated from the intercept

of the real axis in the high-frequency range were almost identical for both cells. However, the total interfacial resistance (R_i) estimated from the summation of R_f and R_{ct} was lower in the cell with the liquid electrolyte. After 300 charge–discharge cycles, the charge transfer resistance dramatically increased in the liquid electrolyte-based cell, as shown in Fig. 5(b). Additionally, the electrolyte resistance in this cell increased slightly after cycling, which may have been caused by exudation of the electrolyte solution. These results suggest that in-situ cross-linking of the electrolyte solution was very effective in maintaining good interfacial contact between the electrodes and the electrolyte, as well as holding the electrolyte solution in the cell. As a result, the cell with cross-linked gel polymer electrolyte exhibited a more stable performance compared with the liquid electrolyte-based cell.

The surface of the carbon negative electrodes cycled in different electrolytes was analysed by XPS measurements, and the results are shown in Fig. 7. Note that the highly resistive LiF, observed at 56.2 eV for Li 1s and 685.0 eV for F 1s [29,30], was more abundant on the electrode surface of the cell with the liquid electrolyte. It is well known that LiF is an insulating material for both electrons and Li^+ ions; thus, the LiF on the surface of the electrode hampered the charge transfer reaction between the electrode and the electrolyte, resulting in an increase in the charge transfer resistance of the liquid electrolyte-based cell. On the other hand, the intensity of the lithium alkyl carbonate ($ROCO_2Li$) that appeared at 532.2 eV for O 1s and 55.0 eV for Li 1s
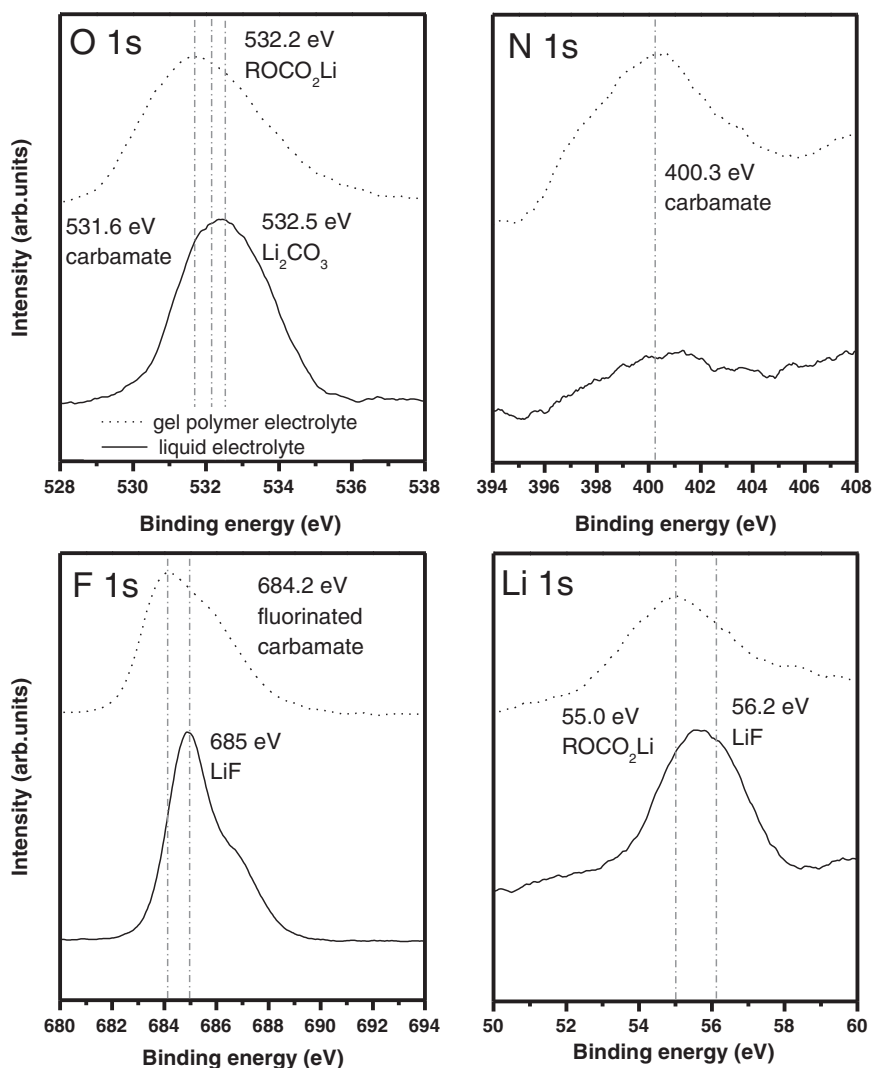

Fig. 7. XPS spectra of the surface for carbon negative electrodes cycled in different electrolytes.

was stronger on the electrode surface in the cell with the gel polymer electrolyte. This result indicates that the SEI formed on the carbon electrode in the cell with the gel polymer electrolyte is less resistive because lithium alkyl carbonate is one of the components in the ion-conducting SEI layer [31]. The peaks corresponding to fluorinated carbamate were observed at 531.6 eV for O 1s, 400.3 eV for N 1s, and 684.2 eV for F 1s [32,33]. It has been reported that fluorinated carbamate plays an important role as a $LiPF_6$ stabiliser [34]. Accordingly, the fluorinated carbamate in the cross-linked gel polymer electrolyte was very effective in weakening the reactivity of PF_5 towards various components in the SEI layer.

$$Li_2CO_3 + PF_5 \rightarrow POF_3 + 2LiF + CO_2$$

$$RCO_2Li + PF_5 \rightarrow RCOF + LiF + POF_3$$

$$ROCO_2Li + PF_5 \rightarrow RF + LiF + CO_2 + POF_3$$

As shown by the above reactions, the SEI components such as Li_2CO_3, RCO_2Li and $ROCO_2Li$ decompose into LiF on the electrode surface by PF_5 [35]. Thus, the battery cycled in the gel polymer electrolyte containing fluorinated carbamate exhibited stable interfacial characteristics by suppressing the above reactions via PF_5.

Fig. 8(a) compares the discharge capacities of the batteries assembled with different electrolytes for various C rates, increasing from 0.2 to 2.0C every five cycles. Fig. 8(b) shows the discharge curves of the batteries with gel polymer electrolytes, which were obtained at the first cycle for every C rate. It can be seen that the use of gel polymer electrolyte prepared by in-situ chemical cross-linking improved the high rate performance. This result can be ascribed to efficient ionic conduction in the gel polymer electrolyte and favourable interfacial charge transport between the electrodes and the electrolyte in the cell, as explained in Fig. 6. The improvement of cycling performance by using gel polymer electrolytes has been also reported previously, which arises from more moveable Li^+ ions and low polarization [36,37].

A cycling test was performed at 55 °C to evaluate the cycling stability of the batteries at high temperatures. There was little difference in the initial discharge capacities between the batteries assembled with different electrolytes, as shown in Fig. 9(a). However, the battery with the liquid electrolyte suffered from severe capacity fading with cycling. From the AC impedance spectra after 100 cycles (Fig. 9(b)), both R_f and R_{ct} were much larger in the liquid electrolyte-based battery. This was due to the fact that the cross-linked polymer network on the electrode surface served as an ion-conductive protection layer to prevent harmful interfacial side reactions between the electrodes and the electrolyte. Our results implied that in-situ cross-linking of liquid electrolyte effectively achieved good capacity retention, high rate performance and cycling stability at high temperature in lithium-ion
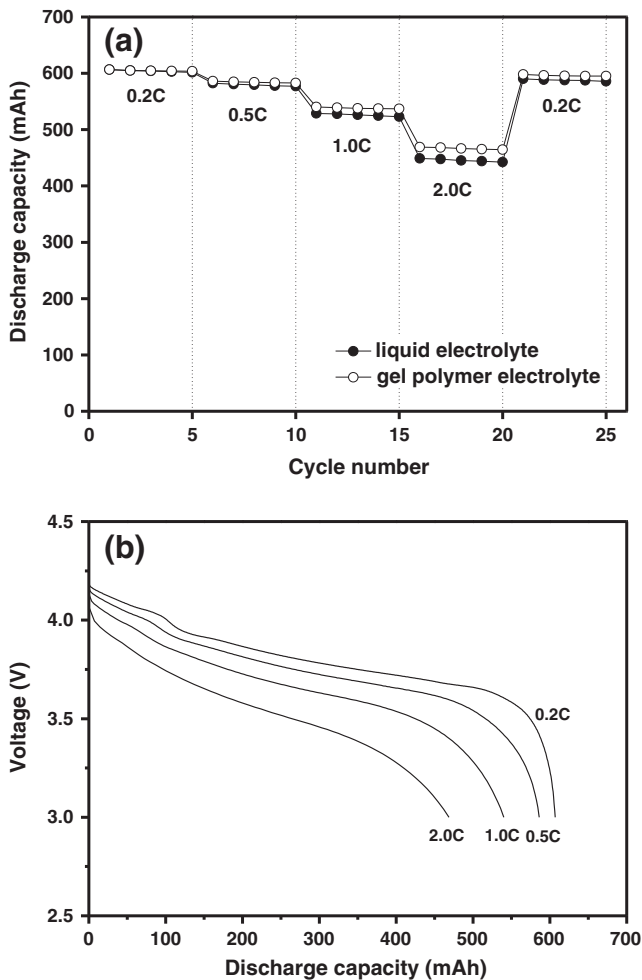

Fig. 8. (a) Discharge capacities of the batteries with liquid electrolyte and cross-linked gel polymer electrolyte, as a function of the C rate, and (b) discharge profiles of the lithium-ion polymer battery assembled with the cross-linked gel polymer electrolyte at different C rates.
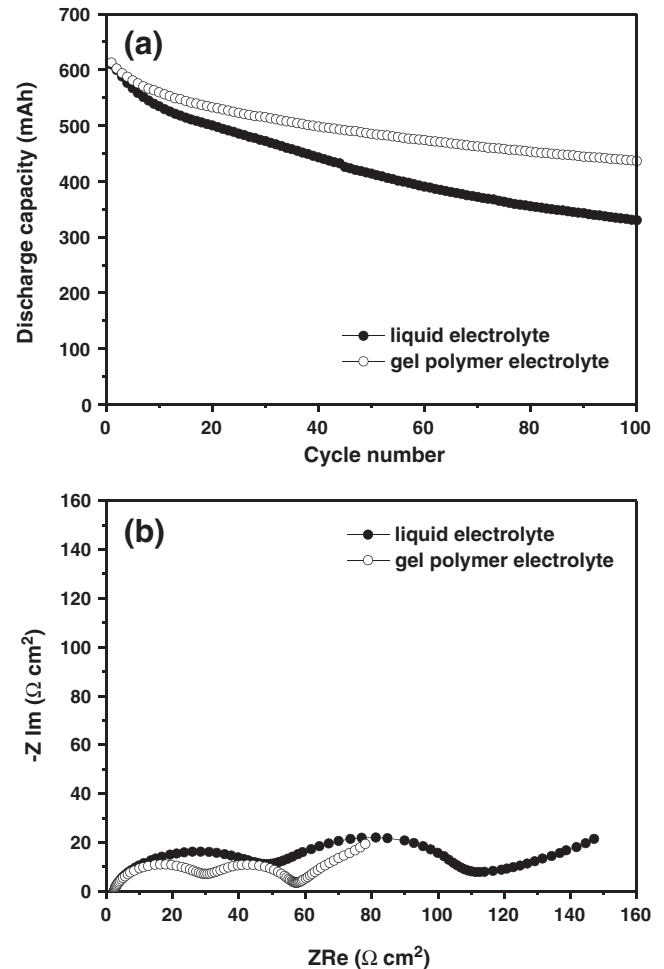

Fig. 9. (a) Discharge capacity as a function of the cycle number and (b) AC impedance spectra after 100 cycles for batteries assembled with the liquid electrolyte and cross-linked gel polymer electrolyte at 55 °C.

polymer batteries, thereby making them superior to lithium-ion batteries with liquid electrolytes.

4. Conclusions

Lithium-ion polymer batteries were assembled with gel polymer electrolytes cured by in-situ chemical cross-linking using a mixture of PEI and PEGDE in an FEC-containing liquid electrolyte. The gel electrolyte precursor could easily penetrate into the cell due to its low viscosity comparable to that of the liquid electrolyte. The chemical cross-linking reaction occurred without any initiators, which promoted strong interfacial adhesion between the electrodes and the separator. Consequently, the batteries assembled using in-situ cross-linking exhibited an improved capacity retention and good rate capability. Thus, gel polymer electrolytes cured by in-situ chemical cross-linking are promising electrolytes for use in rechargeable lithium-ion polymer batteries in emerging applications, such as electric vehicles and energy storage systems.

Acknowledgement

References

[1] Z. Yang, J. Zhang, M.C.W. Kintner-Meyer, X. Lu, D. Choi, J.P. Lemmon, J. Liu, Chem. Rev. 111 (2011) 3577–3613.
[2] M.M. Thackeray, C. Wolverton, E.D. Isaacs, Energy Environ. Sci. 5 (2012) 7854–7863.
[3] M.B. Armand, Solid State Ionics 69 (1994) 309–319.
[4] W.H. Meyer, Adv. Mater. 10 (1998) 439–448.
[5] J.Y. Song, Y.Y. Wang, C.C. Wan, J. Power Sources 77 (1999) 183–197.
[6] J.-M. Tarascon, M. Armand, Nature 414 (2001) 359–367.
[7] G.B. Appetecchi, F. Croce, R. Marassi, S. Panero, F. Ronci, G. Savo, B. Scrosati, Solid State Ionics 143 (2001) 73–81.
[8] H. Tokuda, M. Watanabe, Electrochim. Acta 48 (2003) 2085–2091.
[9] Q. Li, T. Itoh, N. Imanishi, A. Hirano, Y. Takeda, O. Yamamoto, Solid State Ionics 159 (2003) 97–109.
[10] A.S. Arico, P. Bruce, B. Scrosati, J.-M. Tarascon, W. Van Schalkwijk, Nat. Mater. 4 (2005) 366–377.
[11] K. Murata, S. Izuchi, Y. Yoshihisa, Electrochim. Acta 45 (2000) 1501–1508.
[12] K.H. Lee, K.H. Kim, H.S. Lim, J. Electrochem. Soc. 148 (2001) A1148–A1152.
[13] Z. Wen, T. Itoh, T. Uno, M. Kubo, O. Yamamoto, Solid State Ionics 160 (2003) 141–148.
[14] Y. Kang, J. Lee, J.-I. Lee, C. Lee, J. Power Sources 165 (2007) 92–96.
[15] J. Reiter, R. Dominko, M. Nadherna, I. Jakubec, J. Power Sources 189 (2009) 133–138.
[16] J.A. Choi, Y.K. Kang, H.J. Shim, D.W. Kim, E.H. Cha, D.W. Kim, J. Power Sources 195 (2010) 6177–6181.
[17] S.S. Hwang, C.G. Cho, H. Kim, Electrochem. Commun. 12 (2010) 916–919.
[18] M.H. Ryou, Y.M. Lee, K.Y. Cho, G.B. Han, J.N. Lee, D.J. Lee, J.W. Choi, J.K. Park, Electrochim. Acta 60 (2012) 23–30.
[19] S.J. Lim, Y.S. Kang, D.W. Kim, Electrochem. Commun. 12 (2010) 1037–1040.
[20] S.J. Lim, Y.J. Choi, K.S. Song, D.W. Kim, Electrochem. Commun. 13 (2011) 1284–1287.
[21] S. Pinchas, D.B. Ishai, J. Am. Chem. Soc. 79 (1957) 4099–4104.
[22] E. Didier, D.C. Horwell, M.C. Pritchard, Tetrahedron 48 (1992) 8471–8490.
[23] V. Acharya, C.R. Prabha, C. Narayanamurthy, Biomaterials 25 (2004) 4555–4562.
[24] P. Tundo, M. Selva, Acc. Chem. Res. 35 (2002) 706–716.
[25] D. Chaturvedi, Tetrahedron 68 (2012) 15–45.
[26] P. Martin, J. Devaux, R. Legras, M.V. Gurp, M.V. Duin, Polymer 42 (2001) 2463–2478.
[27] A. Funabiki, M. Inaba, Z. Ogumi, J. Power Sources 68 (1997) 227–231.
[28] M.D. Levi, G. Salitra, B. Markovsky, H. Teller, D. Aurbach, U. Heider, L. Heider, J. Electrochem. Soc. 146 (1999) 1279–1289.
[29] D. Aurbach, K. Gamolsky, B. Markovsky, Y. Gofer, M. Schmidt, U. Heider, Electrochim. Acta 47 (2002) 1423–1439.
[30] D. Aurbach, I. Weissman, A. Schechter, Langmuir 12 (1996) 3991–4007.
[31] D. Aurbach, B. Markovsky, A. Shechter, Y. Ein-Eli, H. Cohen, J. Electrochem. Soc. 144 (1996) 3809–3820.
[32] P.R. Davies, J.M. Keel, Surf. Sci. 469 (2000) 204–213.
[33] M. Toselli, M. Messori, R. Bongiovanni, G. Malucelli, A. Priola, F. Pilati, C. Tonelli, Polymer 42 (2001) 1771–1779.
[34] S.S. Zhang, J. Power Sources 162 (2006) 1379–1394.
[35] K. Tasaki, A. Goldberg, J.J. Lian, M. Walker, A. Timmons, S.J. Harris, J. Electrochem. Soc. 156 (2009) A1019–A1027.
[36] Y. Zhu, S. Xiao, Y. Shi, Y. Yang, Y. Wu, J. Mater. Chem. A 1 (2013) 7790–7797.
[37] Y. Zhu, F. Wang, L. Liu, S. Xiao, Z. Chang, Y. Wu, Energy Environ. Sci. 6 (2013) 618–624.